EXPERIMENTAL STUDY ON NOVEL PULSATING HEAT PIPE RADIATOR FOR HORIZONTAL CPU COOLING UNDER DIFFERENT WIND SPEEDS

by

Fumin SHANG[a,b], Qingjing YANG[a*], Shilong FAN[a], Chaoyue LIU[a], and Jianhong LIU[a]

[a] Changchun Institute of Technology, School of Energy and Power, China Changchun, China
[b] Jilin Engineering Research Center for Building Energy Supply and Indoor Environmental Control, China Changchun, China

Original scientific paper
https://doi.org/10.2298/TSCI200729059S

Herein, a horizontal CPU cooler with a pulsating heat pipe for cooling desktop computer was developed. In the experiment, an electric heating block was used to heat a copper plate to simulate the heating process of CPU. The cooling system consists of a cooling fan and a pulsating heat pipe cooler. The influence of cooling wind speed and heat load on heat transfer performance, start-up performance, and temperature uniformity of the pulsating heat pipe cooler was analyzed by controlling variable method. The wind speed was set to be 0 m/s, 0.1 m/s, 0.3 m/s, 0.5 m/s, and 0.7 m/s, respectively. The contour plots were used to analyze the uniformity of temperature distribution due to cooler. The results show that the start-up of the pulsating heat pipe led to a decrease in temperature of CPU. As the cooling wind speed increased, the start-up time of the pulsating heat pipe dropped, the start-up temperature dropped, and its stability was also improved. The operation at different cooling wind speeds also changed the start-up mode of the pulsating heat pipe. The start-up performance was best at cooling wind speed of 0.3 m/s. The contour plot for temperature showed that the temperature distribution of the pulsating heat pipe cooler became more uniform with increased cooling wind speeds. There was excellent temperature uniformity at the cooling wind speeds of 0.3 m/s and 0.7 m/s. When the cooling wind speed was 0.7 m/s, the minimum average thermal resistance was 0.51 K/W.

Key words: *pulsating heat pipe, CPU cooler, cooling wind speed, temperature uniformity, heat transfer performance*

Introduction

With the advent of the period of big data, the development of electronic components to miniaturization and high integration, computing power, and integration of computers are constantly improving. Meanwhile, also increased the CPU power consumption, and even will reduce its service life [1, 2]. The most widespread means of cooling components of CPU, which is one of the largest internal cooling components of PC, is a cooling device consisting of a fan and a radiator to remove heat. The heat-flow of microprocessors will continue to rise, and thermal management is still a tremendous challenge. Especially for some high power electronic equipment, the heat-flow density of local hot spot is 1000 W/cm^2 [3, 4]. Under such a trend, the

* Corresponding author, e-mail: yqjwgj32@126.com

heat-flow level of some electronic equipment will reach 2500 W/cm^2 or higher in the future. Therefore, with the improvement of PC performance, the heat dissipation must be effectively improved. The development of excellent performance radiator is also a global research hot spot [5, 6].

Heat pipe is a kind of passive radiator with stable operation and high heat transfer efficiency. As an efficient heat transfer element, it is often selected for electronic heat dissipation. Extensive research has been performed in the field of heat pipe technology applied [7] to CPU efficient heat dissipation by many scholars. Choi *et al.* [8], Vasiliev [9], Singh *et al*. [10], Harmand *et al*. [11], and Rittidech *et a*l. [12] demonstrate the potential applications of heat pipe technology to improve the efficiency of data centres. As discussed by Kim *et al.* [13], heat pipe for electronics applications was first introduced in personal desktop computers for CPU cooling. The majority of modern computers deploy heat pipes for cooling of CPU, Reay *et al.* [14], which is a promising means to meet the thermal management challenges in the future, Pastukhov [15] and Xie *et al*. [16]. However, the traditional heat pipe is limited in the application of CPU heat dissipation. It cannot contact with the plane heating element directly, which increases the contact thermal resistance, and the compression deformation of the heat pipe affects the operating parameters in the pipe.

In the 1990's, the pulsating heat pipe (PHP) proposed by Akachi [17] had better heat transfer capability than a traditional heat pipe. The technology relies on the characteristics of small size and surface tension heat the working medium in the pipe to oscillate continuously under the thermal driving force in the tube. Hence, the transfer of heat is achieved between the evaporating section and condensing section. It has good heat transfer performance and a simple structure without a wick. The application of PHP to electronics heat dissipation is one of the most potentially useful thermal management topics in the field of electronic equipment. Compared with the traditional heat pipe, in PHP, direct contact with electronic components can be achieved to reduce contact thermal resistance and can be bent optionally without affecting the operating parameters. Improved cooling methods are highly valued for electronics [18-20].

In the research works for applications of PHP in CPU heat dissipation, Maydanik *et al.* [21] proposed a compact cooler for electronics on the basis of PHP and studied the influence of different working mediums on heat transfer performance of radiator. Yang *et al.* [22] designed an aluminum plate closed-loop PHP radiator and conducted a comparative experiment on the effect of different fill ratios of working fluid on the heat transfer performance of the radiator. Rittidech *et al.* [23] made a compact CPU cooler with a closed-end oscillating heat pipe and used it with a fan to conduct cooling experiments on the Pentium4 CPU. They demonstrated the relationship between the heat transfer performance of the cooler and the fan speed. With the increased fan speeds, the heat transfer performance increased. Hemadri *et al.* [24] proposed a thermal radiator with embedded PHP and used infrared camera and numerical simulations to study the effect of the change in inclination on its heat transfer performance. Dang *et al.* [25] proposed a rack concept using PHP for cooling CPU and explored the influence of cooling wind speeds on heat transfer performance of the cooler. With the increase in cooling wind speed, the surface temperature of the CPU decreased. Also, the PHP can be started up quickly to effectively cool electronic chip. Guowei *et al.* [26] conducted an experimental study on a novel heat pipe cooler for vertical CPU cooling and analyzed the influence of heat load, cooling wind speed, and other parameters on the heat transfer performance and start-up performance of the cooler. They found that the radiator delivered stable operation and fast starts. Although there are several studies on the application of PHP in CPU heat dissipation, the concept of using PHP in CPU heat dissipation is still novel. These works

have not explored in detail the effect of wind speed on the heat dissipation of PHP. Herein, we have designed a novel PHP radiator for horizontal CPU cooling followed by a detailed analysis.

The past research works have mainly focused on cooler types, different filling ratio, working fluid, and so on. The study of the start-up performance and temperature uniformity of the cooler is also critical [27, 28]. The PHP shows efficient heat transfer performance after starting-up, which has been studied by many scholars. Qu *et al*. [29] and Xu *et al*. [30] discussed the start-up and steady thermal oscillation of a PHP. Guowei *et al*. [26] proposed that as the heating power increases, the start-up and the stability performance of the PHP become better. Among these, uneven distribution of CPU surface temperature also has a great impact on the CPU performance. Herein, the experiments mainly studied the start-up performance of PHP coolers at different cooling wind speeds. Also, the temperature uniformity of the cooler has been investigated using contour diagrams [31]. The heat transfer performance was also analysed in terms of thermal resistance.

Experiment set-up

Experimental equipment

The experimental system, fig. 1, consisted of three parts, namely the heating, the cooling, and the data acquisition system. The heating system consisted of transformers, an ammeter, a voltmeter, a heating block, and a copper plate, as shown in fig. 1.

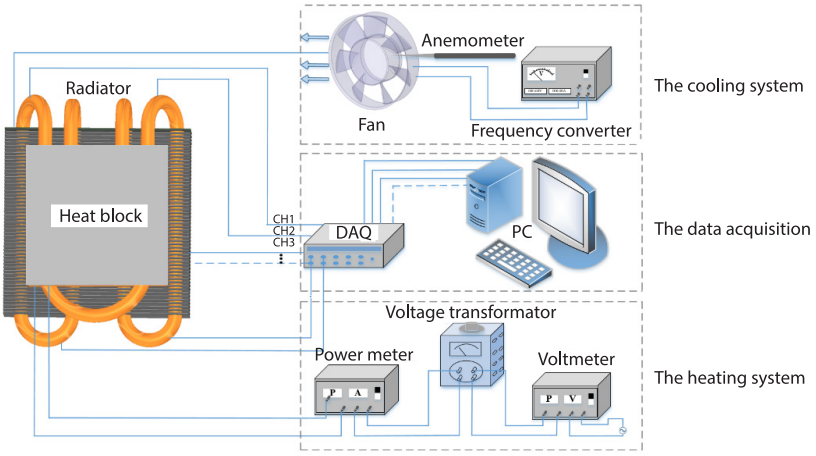

Figure 1. Experiment system diagram

A 60 × 60 mm copper plate was heated by the heating block to simulate the heat load from a CPU. The upper and lower sides of the copper plate were assembled together with heating block to form the main body of the heating system. Between the copper plate and heat sink, the heating plate was coated with thermally conductive silicone to reduce the contact thermal resistance. The heating block was insulated with insulating cotton reduce the heat loss. The size of the heating block was the same as that of the copper plate. Its maximum heat load was 200 W, and heat load was varied by adjusting the transformer. The cooling system consisted of a fan with variable frequency to enhance the convection cooling of the heat exchanger. The cooling wind speed was collected with the JTR07B hot-wire anemometer with ±(0.3 m/s +0.4%) accuracy. The air duct, fig. 2 is a rectangular duct. The hot-wire anemometer

is used to measure the wind speed at different positions in the same cross-section, and the average value is calculated as the wind speed in a certain state.

The data acquisition system adopted a *K*-type thermocouple (with the measurement error is ±4 ℃, and he temperature range is 0~1300 ℃.) for real-time monitoring of the wall temperature data of the PHP cooler and data was collected using Agilent 34972A data collector with 0.4% accuracy. The temperature data was transmitted to the computer for processing and storage. The thermocouple used to measure the temperature of the heating block was installed at the contact surface between the heating block and the heat sink (T1-T5). Two thermocouples (T6, T7) were installed on the adiabatic section and two more were installed on the condensing segment (T8, T9). The lay-out of the instrumented points is shown in fig. 3.

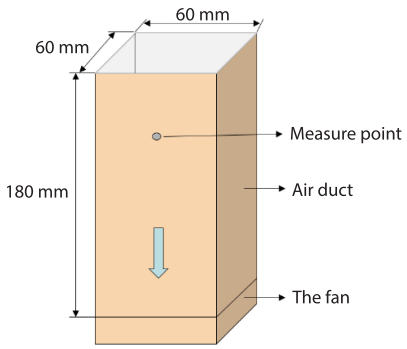

Figure 2. The air duct

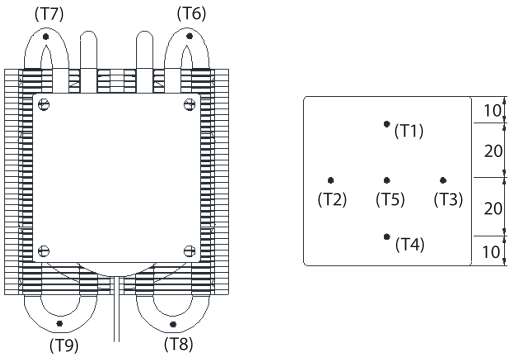

Figure 3. The thermocouples' locations

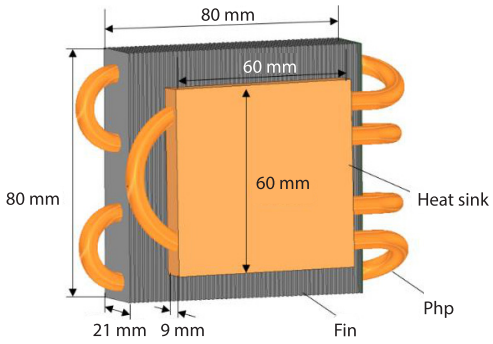

Figure 4. The structure a of the PHP CPU cooler

The PHP cooler was mainly composed of the PHP, a cooling fin array which is the heat sink, and a fan, as shown in fig. 4. The PHP consisted of a copper tube with a length of 731 mm, an inner diameter of 2 mm, and an outer diameter of 4 mm, bent into pattern with two turns. The outside of the heat pipe's condenser section was equipped with aluminum fins to increase its heat dissipation area and cooling. The geometric parameters of the PHP cooler are listed in tab. 1. A PHP have different start-up and oscillation characteristics with regards to different working fluids. Herein, the working fluid was deionized water with a 50% filling ratio. While filling it with the working fluid, the fine copper welded fluid-filled pipe was connected with the vacuum pump. After filling it with the working fluid under high vacuum, the liquid was sealed into the copper tube.

Table 1. Geometrical parameters of the cooler

Outer diameter [mm]	Inner diameter [mm]	Heat sink structure [mm]	The structure of each fin [mm]	Spacing of fins
4	2	60 × 60 × 9	80 × 21 × 0.2	2

Experimental procedure

The influence of cooling wind speed on heat transfer characteristics of PHP cooler was studied. As previously mentioned, it has been proved by a lot of previous studies [32-34], when the liquid filling ratio of the PHP was 50%, the PHP has excellent heat transfer and start-up performance characteristics. Therefore, the PHP cooler with a 50% liquid filling ratio was adopted.

For the experiment, the specific cooling wind speed was first set to 0 m/s and the heat load was 5 W. In order to enable the PHP to fully operate in each group of working conditions, after the heat pipe reached a steady-state, the input heat was gradually increased by 5 W per step each time until the final heat load of 55 W was reached (when heating to 55 W, the evaporation section temperature has exceeded 80 ℃, the surface temperature at which the CPU can safely operate should not exceed 80 °C, it is meaningless to continue to increase the power). The experimental time for each group of input heat was 30 minutes. After the end of one set of experiments, the PHP was allowed to cool to a steady-state in a room temperature environment at 25 °C. Before the start of the next set of experiments, the PHP was shaken to distribute the working fluid randomly in the tube to avoid the influence of the previous set of experiments. Experiments were performed with the cooling wind speeds of 0 m/s, 0.1 m/s, 0.3 m/s, 0.5 m/s, and 0.7 m/s. Among these, 0 m/s was taken as the base case condition for this experiment.

Results and discussion

Thermal resistance is a significant evaluation metric to measure the heat transfer capability of a PHP (the evaporation section was embedded in the heat sink, and will be using the adiabatic section calculate the thermal resistance). The heat dissipation performance increased with the decrease in thermal resistance. The equations of thermal resistance are:

$$R = \frac{T_a - T_c}{Q_{\text{in}}} \tag{1}$$

$$T_a = \frac{1}{2}\sum_{1}^{2} T_{ai} \tag{2}$$

$$T_c = \frac{1}{2}\sum_{1}^{2} T_{ci} \tag{3}$$

where R is the operating thermal resistance, T_a – the average temperature of the adiabatic section, T_c – the average temperature of the condensation section, and Q_{in} – the input power to the heating block.

Based on the experimental method and the operational characteristics of the PHP, the first large temperature oscillation in the evaporation section was defined as PHP start-up. The start-up temperature is the instantaneous temperature of the evaporation section when the PHP starts up, and the start-up time is the time lag from the beginning of the experiment to the start-up of the PHP.

As the PHP cooler is in direct contact with the CPU, the temperature distribution of the heated end impacts the temperature of the CPU chip. If there are excessive *hot spots* on the surface of the CPU, the performance of the CPU would be reduced, or it can even lead to damage. For the study of *hot spots* phenomena, the temperature uniformity of the evaporation section was used to study the temperature distribution during the operation of the PHP. Combined with the analysis of contour plot, the temperature uniformity of the PHP CPU cooler is explained.

The uncertainty is divided into direct measurement and indirect measurement parameters. Among them, T is the uncertainty of direct measurement, Q and R are the uncertainties of indirect measurement:

$$Q = U \times I \tag{4}$$

The uncertainties of direct measurement and indirect measurement can be expressed [35]:

$$u=\sqrt{u_r^2+u_s^2} \tag{5}$$

$$u(N)=\sqrt{\left[\frac{\partial f}{\partial x}u(x)^2\right]+\left[\frac{\partial f}{\partial y}u(y)^2\right]+\left[\frac{\partial f}{\partial z}u(z)^2\right]+\ldots} \tag{6}$$

Then:

$$\frac{\partial Q}{Q}=\sqrt{\left(\frac{\mathrm{d}U}{U}\right)^2+\left(\frac{\mathrm{d}I}{I}\right)^2} \tag{7}$$

$$\frac{\partial R}{R}=\sqrt{\left(\frac{\partial T_a}{T_a-T_c}\right)^2+\left(\frac{\partial T_c}{T_a-T_c}\right)^2+\left(\frac{\partial Q}{Q}\right)^2} \tag{8}$$

where u_s is the system uncertainty and u_r – the random uncertainty. Through analysis of the uncertainty and the aforementioned definition, the uncertainty of the indirectly measured parameters such as Q and R were obtained. The voltage and current of power supply have accuracies both of 0.5, and the uncertainty generated by temperature measurement can be calculated by thermocouple precision. The maximum uncertainties of main parameters are presented in tab. 2.

Table 2. Maximum uncertainties of main parameters

Parameters	T_a	T_c	Q	R
Uncertainty (±)	0.7%	0.7%	5.03%	5.64%

Effects of cooling wind speed on start-up time and temperature

The temperature measurement points T6 and T8 are the corresponding temperature measuring points of the evaporation and condensed sections. Based on the temperature changes of T6 and T8, the profile wall temperature changes are displayed in fig. 5. During the start-up process, the working fluid in the evaporation section of the PHP starts to oscillate, but the temperature oscillation in the condensation section is not clear. Therefore, the start-up performance of the PHP was studied using the temperature oscillation data from the evaporation section.

The operation process of a PHP has different states. First, at low heat loads, the temperature profile rises smoothly with the increasing heat input. Then, the working fluid begins to oscillate, the temperature in the evaporation section drops suddenly, and the condensation section's temperature rises abruptly, and the PHP starts to start-up. Finally, after experiencing the first temperature oscillation, the PHP entered its stable operation stage.

Figure 5 shows the wall temperature profile variation diagram of the PHP cooler start-up process under different cooling wind speeds. In the figure, the cooling wind speed has an important influence on operation mode of the PHP.

Figure 5(a) shows the wall temperature data plotted when the cooling wind speed was 0 m/s, the initial start-up period of the PHP was 6705 seconds, and the highest temperature was 80.9 °C. The cooler did not effectively ensure that the CPU was adequately cooled at this cool-

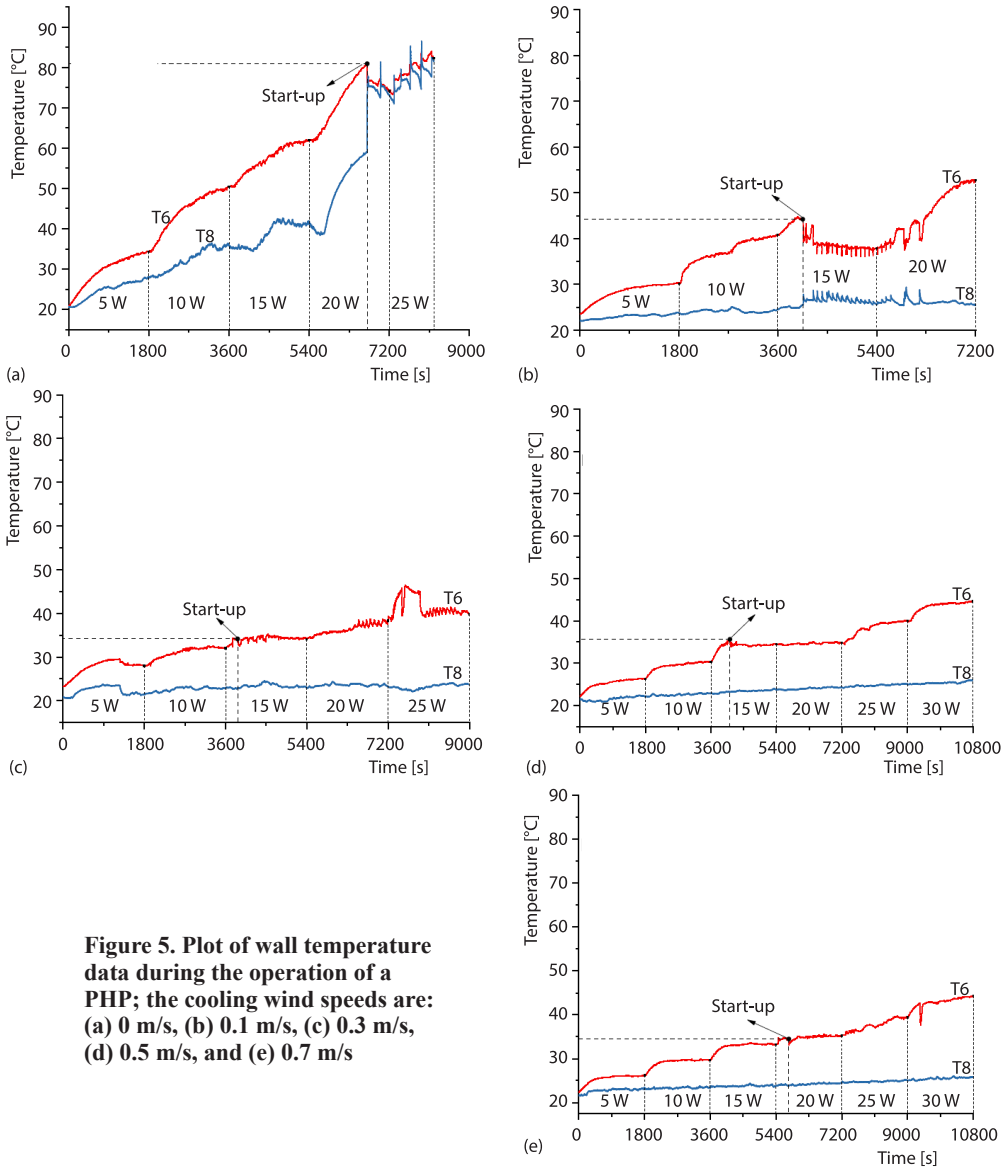

Figure 5. Plot of wall temperature data during the operation of a PHP; the cooling wind speeds are: (a) 0 m/s, (b) 0.1 m/s, (c) 0.3 m/s, (d) 0.5 m/s, and (e) 0.7 m/s

ing wind speed, without increased forced convection. With increased heat load, the temperature in the evaporation section rose rapidly and heat accumulated. The temperature difference between the cold and hot sections gradually dropped. The working fluid did not have enough driving force to move itself, and the PHP had difficulty in starting and could not transfer heat into the air effectively. Therefore, with a cooling wind speed of 0 m/s, cooler is not useful for CPU heat dissipation. Figure 5(b) shows the wall temperature plot for the cooling wind speed of 0.1 m/s. The start-up time at this cooling wind speed was 2649 seconds shorter than that at 0 m/s, and the temperature was lower by 36.2 °C. The increase in cooling wind speed had a significant impact on the start-up process of the PHP. Figure 5(c) shows the wall temperature plot for a cooling wind speed of 0.3 m/s. The PHP start-up time was now at its shortest

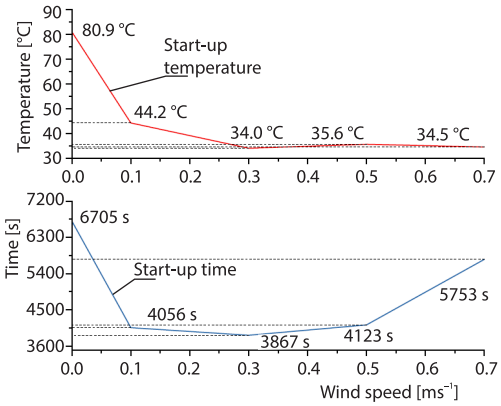

Figure 6. Start-up time and temperature of PHP

and its start-up temperature was at its lowest, at only 34.0 °C. The start-up performance was the best in this working condition. With increased heat load, the pressure in the condenser section was reduced, the pressure difference between the adiabatic and condensation sections was increased, and the flow of the working fluid in the channel was induced to move from the evaporation section the condenser section. Thus, the pressure between the adjacent channel was released and the start-up performance was improved. Hence, the change in heat load had a relatively clear impact on the start-up response in terms of time and temperature. Figures 5(d) and 5(e) show the wall temperature plot for as the cooling wind speeds of 0.5 m/s and 0.7 m/s. The start-up time and temperature at different cooling wind speeds are listed in fig. 6. As can be seen from fig. 6, with the increase in heat load, the start-up temperature drops, and the PHP starts more easily.

Effects of cooling wind speed on the start-up mode

In figs. 5(a) and 5(b), the cooling wind speeds are 0 m/s and 0.3 m/s, respectively. It can be seen from the PHP wall temperature profile that T6 and T8 start simultaneously. After the PHP started working, the profile had a clear sustained oscillation, with a high oscillation frequency and a small amplitude. When the cooling wind speed was low, the heat transfer performance of the PHP improved with increased power, which is conductive to reaching the stable oscillation phase of the PHP. After entering the stable oscillation stage, T6 and T8 could still maintain the synchronous oscillation trend. The reason for this phenomenon is that with continuous heat input and low cooling wind speeds, the pressure difference between the heated section and the cooled section of the same channel can be maintained consistent, and the pressure difference between the adiabatic and condensation sections can be kept at about the same value. Thus, T6 and T8 can see stable oscillations simultaneously. From figs. 5(c)-5(e), the start-up mode of T6 and T8 was partial start, the start-up times were different, and T6 starts before T8. After the PHP started up, instead of moving directly into the stable oscillation phase, it saw an intermittent oscillation (the phenomenon of intermittent oscillation is the repeated *stop-start* after the PHP is started-up, it is caused by uneven distribution of vapour and liquid phase between adjacent channels and insufficient input heat load). Moreover, the oscillation frequency was low and with a lager amplitude. When the cooling wind speeds are 0.3 m/s, 0.5 m/s, and 0.7 m/s, respectively, the analysis shows that with increased cooling wind speeds, the input heat load was insufficient and the vapour and liquid phase distribution between the adjacent pipe-lines was uneven. The instability of the oscillation led to accumulation of heat in the evaporation section and failure of the PHP to rapidly transfer heat to the condensation section. When the system was run at low cooling wind speed, the PHP had stable oscillations, which are reliable for stable and effective heat dissipation from a CPU. When operated at high cooling wind speeds, intermittent oscillations could reduce the pressure in the hot section and help the condensing section reflux and prevent dryout in the evaporation section, but these lack persistence and stability. Combined with the aforementioned analysis, changes in cooling wind speed can change a PHP start-up characteristics.

Analysis of temperature uniformity

Figure 6 displays a contour plot of the temperature ratio, drawn according to the distance temperature measurement points at different positions of T1, T4, and T5, at different cooling wind speeds. The horizontal axis is the distribution distance of T1, T4, and T5 temperature measuring points. The T1 is located at 10 mm, T4 at 30 mm, and T5 at 50 mm. The vertical is the heat load variation, and the contour value is the temperature. Figure 7 shows the wall temperature profile for T6 and T8, for different cooling wind speeds. As the copper plate is square and has symmetric structure, the temperature distribution of the three temperature measurement points (T1, T4, and T5, as shown in fig. 2.) on the centerline of the image was selected to study the temperature uniformity of the PHP cooler.

For contour plot, the temperature of the measuring point on the horizontal axis varies with the increase of the heat load on the vertical axis, different temperatures show different colors on the graph. If the temperature of the three measuring points on the contour plot changes along the horizontal axis under the same heat load and all are in the same color level, then the temperature distribution of the three measuring points with different spacing is very uniform and there is no *hot spot*. Therefore, the temperature uniformity of the evaporation section of the PHP cooler is good. On the contrary, in the same heating load, the corresponding transverse temperature change is not in the same color level, indicating that the fluctuating PHP evaporation section under the heating power operation is unstable, temperature uniformity is poor. Therefore, the temperature uniformity of t the PHP cooler can be explored through the temperature changes of the T1, T4, and T5 in the evaporation section.

As shown in fig. 7, the temperature increased with heat load. For the same heat load, the temperature distribution of T1, T4, and T5 was extremely uniform, with a clear temperature boundary distribution. Figure 7(a) shows the contour plot of the temperature at the cooling wind speed of 0 m/s. There were irregular partial fluctuations in the temperature distribution between 25 W and 30 W. In other words, there was a *hot spot* on the cooler. Figure 8(a) presents the wall temperature profile for T6 and T8, for a cooling wind speed of 0 m/s. Combined with the results illustrated in fig. 8(a), it can be observed that the first large temperature jump occurred in the condensation section during the stable oscillation phase. After this phenomenon appeared, as the heat load increased, the amplitude of the temperature profile of T8 increases, while the amplitude of the temperature profile of T_6 did not change significantly. This is due to the structure of the cooler. The ratio between the length of its cold and hot sections and the length of the evaporation section was close to 1. Its heat dissipation capacity was weak in the natural-convection environment without fan-forced air movement. With the increased input heat, the flow resistance of the working fluid in the channel increased and the circulation of the working fluid degraded, causing the temperature of the condensing section rise rapidly. According to aforementioned section *Effect of cooling wind speed on start-up time and temperature* the heat transfer performance of the PHP cooler was the worst when the cooling wind speed was 0 m/s. With increased heat load, the temperature of T8 was higher than it was at T6, and no dryout phenomenon occurred, indicating that the heat transfer limit of the PHP was extremely high.

Figures 7(b) and 8(b) show the distribution of the temperature contour plot and wall temperature profile, respectively, at the cooling wind speed of 0.1 m/s. Figures 7(b) and 8(b) were combined for analysis. As the heat load is 25~35 W, there are the same irregular partial fluctuations as when the cooling wind speed is 0 m/s for the reason as before. Figures 7(d) and 8(d) show the distribution of the temperature contour plot and wall temperature profile with a cooling wind speed of 0.5 m /s, respectively. When the cooling wind speed was 0.5 m /s, and the heat load was 45~50 W, there were also *hot spots*. Furthermore, the temperature range of *hot*

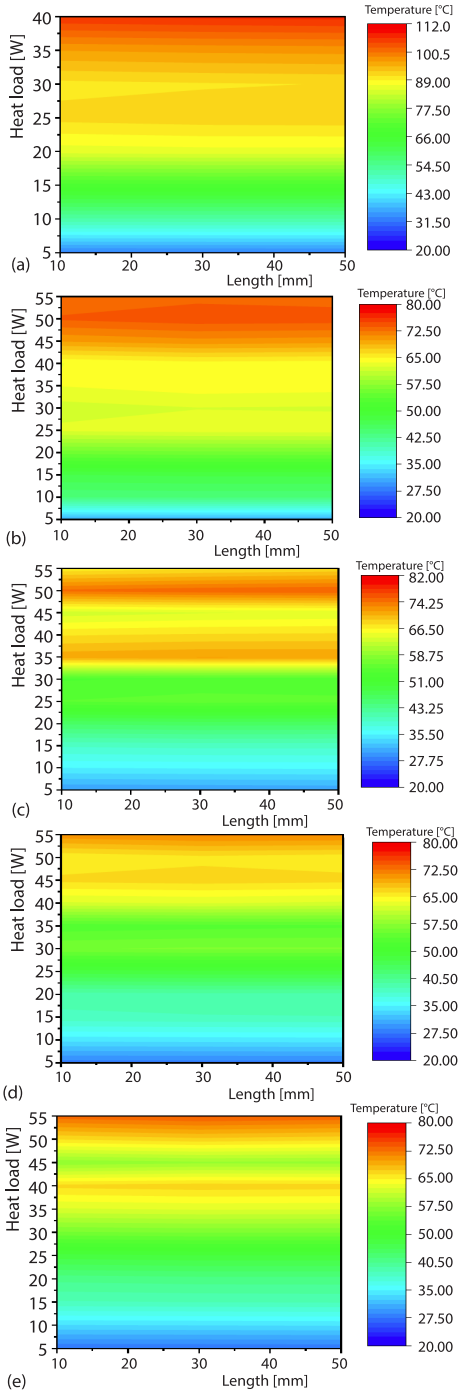

Figure 7. Contour plot of T1, T4, and T5 temperature ratios; the wind speeds are: (a) 0 m/s, (b) 0.1 m/s, (c) 0.3 m/s, (d) 0.5 m/s, and (e) 0.7 m/s

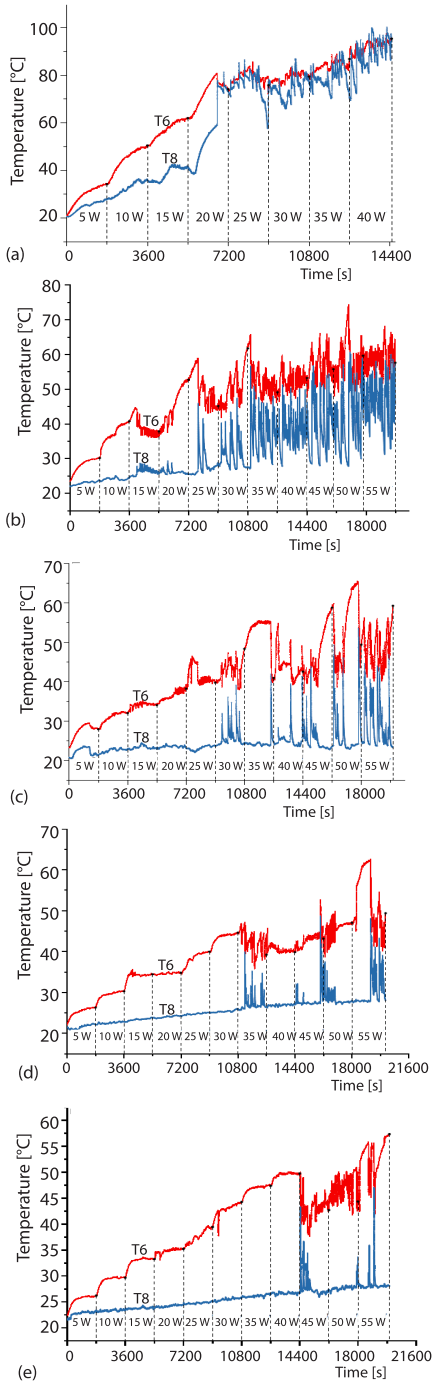

Figure 8. Wall temperature curves of T6 and T8; the wind speeds are: (a) 0 m/s, (b) 0.1 m/s, (c) 0.3 m/s, (d) 0.5 m/s, and (e) 0.7 m/s

spots was larger in fig. 7(b). It can be concluded from the analysis that the cooling wind speed was too low to dissipate heat quickly. Figures 7(c) and 7(e) show the distribution of the temperature contour plots at cooling wind speeds of 0.3 m/s and 0.9 m/s, respectively. In figs. 7(c) and 7(e), there was no irregular partial temperature fluctuation. Therefore, when the cooling wind speeds were 0.3 m/s and 0.7 m/s, the temperature distribution of PHP was more uniform. Also, except at 0 m/s cooling wind speed, the phenomenon of a higher temperature at T8 than at T6 did not occur in the four cooling wind speeds.

To summarize, temperature uniformity is reflected in the effect of the increase in evaporation section temperature from the heat load, resulting in a larger temperature difference in the cold and hot sections and a deteriorating heat transfer environment. The variations of cooling wind speed have a significant influence on the temperature uniformity of the PHP cooler.

Effects of cooling wind speed on heat transfer performance

Figure 9 shows the variation of thermal resistance with different cooling wind speeds. As shown in the figure, the thermal resistance first increased and then decreased with increasing heat loads. Also, when the initial heating power is 5 W, the higher the cooling wind speeds, smaller is the thermal resistance. When the cooling wind speed is 0 m/s, the average thermal resistance was at its maximum of 1.36 K/W. As 5~15 W heating load, the thermal resistance increases, and when the heating load is 15~40 W, the thermal resistance begins to decrease rapidly. When increased to 15 W, the thermal resistance decreased greatly, which was extremely destabilizing for the whole operational process. Figure 10 shows that when the heat load increased to 40 W, the average temperature of the evaporation section was up to about 100 °C, and it was meaningless to further increase the heat load. This is not conducive for the stable operation of the PHP cooler, and the cooler could not work normally. When the cooling wind speed was 0.7 m/s, the average thermal resistance was at its smallest value at 0.51 K/W.

Figure 10 shows the average temperature profile for the evaporation section *vs.* different cooling wind speeds. As the input heat load was increased to 55 W, the maximum average temperatures of the evaporation section corresponding to cooling wind speeds of 0.1 m/s, 0.3 m/s, 0.5 m/s, and 0.7 m/s were about 75 °C, 66 °C, 63 °C, and 53 °C, respectively. Generally, the upper limit to the CPU operating temperature is 80 °C. When the temperature of the evaporation section was less than 80 °C, it indicates that the PHP cooler played an effective role in heat dissipation. In other words, the PHP cooler had a good heat transfer performance and could meet

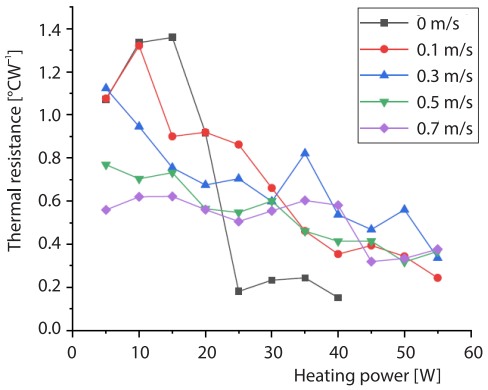

Figure 9. Thermal resistance with different wind speeds

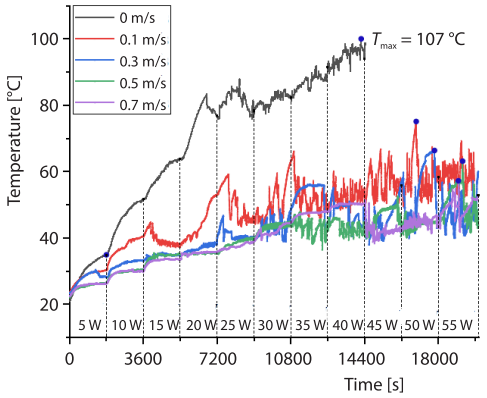

Figure 10. Average temperature in the evaporation section at different wind speed change

the cooling needs of high heat flux electronic chip. When the heat load was 55 W, the maximum temperature reached was 107 °C, and the PHP still operated normally without any dryout.

Conclusions

- With the increase in heat load, the start-up time drops and the temperature is lower. With the increase of wind speed, the PHP starts-up faster. When the cooling wind speed was 0.1 m/s, the start-up time was about 60% less than it was for 0 m/s cooling wind speed, and the start-up temperature was about 55% lower than with 0.1 m/s cooling wind speed. When the cooling wind speed was 0.3 m/s, the start-up time was at its shortest and the start-up temperature was at its lowest, at only 34.0 °C. At this cooling wind speed, the start-up performance was at its best.
- The cooling wind speed had a clear influence on the start-up mode of a PHP. At low cooling wind speeds, with the increasing heat loads, the heat transfer performance of the PHP improved, which is conducive for stable PHP oscillation phases. As running at high cooling wind speeds, intermittent oscillation occurred in PHP operation. Intermittent oscillations can reduce the pressure in the heating section, but this mode lacks stability.
- With increased cooling wind speeds, the temperature uniformity of PHP CPU coolers was better. When the cooling wind speeds were 0.3 m/s and 0.7 m/s, the average temperature distribution of the cooler was uniform and there were no *hot spots*. With cooling wind speeds of 0 m/s, 0.1 m/s, and 0.5 m/s, the *hot spots* appeared in the temperature distribution, potentially affecting the heat transfer performance of the cooler.
- The thermal resistance first increased and then decreased with increased heat load. At the same initial heat load, higher the cooling wind speed, smaller was the thermal resistance. When the cooling wind speed was 0 m/s, the average thermal resistance was at its maximum of 1.36 K/W. The sharp drop of thermal resistance is large and the operation is unstable and the cooling effect was at its worst. When the cooling wind speed was 0.7 m /s, the average thermal resistance was at its minimum at 0.51 K/W.

Acknowledgment

This work was supported by the science and technology development project of Jilin province (Grant No. 20190303113SF) and industrial technology research and development project of Jilin province (2019C057-5).

Nomenclature

a – adiabatic section, [–]
c – condensation section, [–]
I – current, [A]
Q – effective heat input, [W]
R – thermal resistance, [KW^{-1}]
T – temperature, [°C]
U – voltage, [V]
u – uncertainty, [–]
u_r – random uncertainty, [–]
u_s – system uncertainty, [–]

References

[1] Bahiraei, M., Heshmatian, S., Electronics Cooling with Nanofluids: A Critical Review, *Energy Convers Manage*, *172* (2018), 15, pp. 438-456
[2] Zhou, W., *et al*., A Novel Ultra-Thin Flattened Heat Pipe with Biporous Spiral Woven Mesh Wick for Cooling Electronic Devices, *Energy Convers Manage*, *180* (2019), 15, pp. 769-783
[3] Mudawar, I., Assessment of High-Heat-Flux Thermal Management Schemes, *IEEE Transactions on Components and Packaging Technologies*, *24* (2001), 2, pp. 122-141
[4] Hao, X., *et al.,* Efficient on-Chip Hotspot Removal Combined Solution of Thermoelectric Cooler and Mini-Channel Heat Sink, *Applied Thermal Engineering*, *100* (2016), 5, pp. 170-178.

[5] Yang, Cai., *et al.*, Optimization of Thermoelectric Cooling System for Application in CPU Cooler, *Energy*, *Procedia*, *105* (2017), May, pp. 1644-1650
[6] Hemadri, V. A., *et al.*, Thermal Radiators with Embedded Pulsating Heat Pipes: Infra-Red Thermography and Simulations, *Applied Thermal Engineering*, *31* (2011), 6-7, pp. 1332-1346
[7] Wang, J.-C., Superposition Method to Investigate the Thermal Performance of Heat Sink with Embedded Heat Pipes, *International Journal of Heat and Mass Transfe*r, *36* (2009), 7, pp. 686-692
[8] Choi J., *et al.*, A New CPU Cooler Design Based on an Active Cooling Heatsink Combined with Heat Pipes, *Applied Thermal Engineering*, *44* (2012), Nov., pp. 50-56
[9] Vasiliev, L. L., Micro and Miniature Heat Pipes-Electronic Component Coolers, *Applied Thermal Engineering*, *28* (2008), 4, pp. 266-273
[10] Singh, R., *et al.,* Miniature Loop Heat Pipe with Flat Evaporator for Cooling Computer CPU, Components and Packaging Technologies, *IEEE Transactions on*, *30* (2007), 1, pp. 42-49
[11] Harmand, S., *et al.*, Transient Cooling of Electronic Components by Flat Heat Pipes, *Applied Thermal Engineering*, *31* (2011), 11, pp. 1877-1885
[12] Rittidech, S., *et a*l., Correlation Predict Heat Transfer Characteristics of a Closed-end Oscillating Heat Pipe at Normal Operating Condition, *Applied Thermal Engineering*, *23* (2003), 4, pp. 497-510
[13] Kim, K. S., *et al*., Heat Pipe Cooling Technology for Desktop PC CPU, *Applied Thermal Engineering*, *23* (2003), 9, pp. 1137-1144
[14] Reay, D., Harvey, A., The Role of Heat Pipes in Intensified Unit Operations, *Applied Thermal Engineering*, *57* (2013), 1-2, pp. 147-153
[15] Pastukhov, V. G., *et al*., Miniature Loop Heat Pipes for Electronics Cooling, *Applied Thermal Engineering*, *23* (2003), 9, pp. 1125-1135
[16] Xie, X., *et al*., An Experimental Investigation on a Novel High-Performance Integrated Heat Pipe Heat Sink for High-Flux Chip Cooling, *Applied Thermal Engineering*, *28* (2008), 5-6, pp. 433-439
[17] Akachi, H., *Structure of a Heat Pipe*, US Patent# 4991041, 1990
[18] Lim, J., Kim, S. J., Fabrication and Experimental Evaluation of a Polymer-Based Flexible Pulsating Heat Pipe, *Energy Convers Manag*e, *156* (2018), Jan., pp. 358-364
[19] Hsieh, S., Yang, Y., Design Fabrication and Performance Tests for a Polymer-Based Flexible Flat Heat Pipe, *Energy Convers Manage*, *7*0 (2013), June, pp. 10-19
[20] Rong, J. X., *et al*., Experimental Investigation of a Solar Collector Integrated with a Pulsating Heat Pipe and a Compound Parabolic Concentrator, *Energy Convers Manage*, *148* (2017), Sept., pp. 68-77
[21] Maydanik., Y. F., *et al*., Compact Cooler for Electronics on the Basis of a Pulsating Heat Pipe, *Applied Thermal Engineering*, *29* (2009), 17, pp. 3511-3517
[22] Yang, H., *et al*., Performance Characteristics of Pulsating Heat Pipes as Integral Thermal Spreaders, *International Journal of Thermal Sciences*, *48* (2009), 4, pp. 815-824
[23] Rittidech, S., *et al*., Correlation Predictheat Transfer Characteristics of a Closed-end Oscillating Heat Pipe at Normal Operating Condition, *Applied Thermal Engineering*, *23* (2003), 4, pp. 497-510
[24] Hemadri, V. A., *et al*., Thermal Radiators with Embedded Pulsating Heat Pipes: Infra-Red Thermography and Simulations, *Applied Thermal Engineering*, *31* (2011), 6-7, pp. 1332-1346
[25] Chao, D., *et al.*, Investigation on Thermal Design of a Rack with the Pulsating Heat Pipe for Cooling CPU, *Applied Thermal Engineering*, *110* (2016), Jan., pp. 390-398
[26] Guowei, X., *et al.*, Novel Heat Pipe Radiator for Vertical CPU Cooling and Its Experimental Study, *International Journal of Heat and Mass Transfer*, *130* (2019), Mar., pp. 912-922
[27] Liu, P., *et al.*, Heat Transfer Enhancement, Entropy Generation and Temperature Uniformity Analyses of Shark-Skin Bionic Modified Micro-Channel Heat Sink, *International Journal of Heat and Mass Transfer, 146* (2020), Jan., 118846
[28] Liu, H., *et al.*, Heat Transfer and Flow Performance of a Novel T-type Heat Sink with GaInSn Coolant, *International Journal of Thermal Sciences*, *144* (2019), Oct., pp. 129-146
[29] Qu, J., *et al.*, Start-up, Heat Transfer and Flow Characteristics of Silicon-Based Micro Pulsating Heat Pipes, *International Journal of Heat and Mass Transfer*, *55* (2012), 21-22, pp. 6109-6120
[30] Xu, J., *et al.*, Start-up and Steady Thermal Oscillation of a Pulsating Heat Pipe, *Heat and Mass Transfer*, *41* (2005), 8, pp. 685-694
[31] Hoon, T., *et al.*, Closed-Form Correlations of Pressure Drop and Thermal Resistance for a Plate Fin Heat Sink with Uniform Air Jet Impingement, *Energy Conversion and Management*, *136* (2017), Mar., pp. 340-349
[32] Liu, X., *et al.*, Dynamic Performance Analysis on Start-up of Closed-Loop Pulsating Heat Pipes (CLPHP), *International Journal of Thermal Sciences*, *65* (2013), Comp., pp. 224-233

[33] Shafii, M. B., *et al.*, Experimental Investigation of Pulsating Heat Pipes and a Proposed Correlation, *Heat Transfer Engineering*, *31* (2010), 10, pp. 854-861
[34] Verma, B., *et al.*, Experimental Studies on Thermal Performance of a Pulsating Heat Pipe with Methanol/DI Water, *Journal of Electronics Cooling and Thermal Control*, *3* (2013), 1, pp. 27-34
[35] Cui, X., *et al.*, Combination Study of Operation Characteristics and Heat Transfer Mechanism for Pulsating Heat Pipe, *Applied Thermal Engineering*, *65* (2014), 1-2, pp. 394-402

Paper submitted: July 29, 2020
Paper revised: December 14, 2020
Paper accepted: December 25, 2020